



Published in final edited form as:

*J Biomed Opt.* 2009 ; 14(3): 034048. doi:10.1117/1.3139850.

## Multiphoton Adaptation of a Commercial Low Cost Confocal Microscope for Live Tissue Imaging

James J. Mancuso<sup>1</sup>, Adam M. Larson<sup>2</sup>, Theodore G. Wensel<sup>1,2</sup>, and Peter Saggau<sup>2</sup>

Peter Saggau: psaggau@bcm.edu

<sup>1</sup>Verna and Marrs McLean Department of Biochemistry and Molecular Biology, Baylor College of Medicine, One Baylor Plaza Houston, TX 77030

<sup>2</sup>Department of Neuroscience, Baylor College of Medicine, One Baylor Plaza Houston, TX 77030

### Abstract

The Nikon C1 confocal laser scanning microscope is a relatively inexpensive and user-friendly instrument. We describe here a straightforward method to convert the C1 for multiphoton microscopy utilizing direct coupling of a femtosecond near infrared (NIR) laser into the scanhead and fiber optic transmission of emission light to the three-channel detector box. Our adapted system can be rapidly switched between confocal and multiphoton mode, requires no modification to the original system, and uses only a few custom-made parts. The entire system, including scan mirrors and detector box, remain under the control of the user-friendly Nikon software without modification.

### Introduction

Multiphoton laser scanning microscopy (MPLSM) has emerged as a powerful tool in physiological imaging of live tissues. The ability to use long excitation wavelengths (700–1000nm) results in reduced auto-fluorescence of biological tissue and significantly less light scattering (1). In studies involving imaging of living brain tissues, these properties allow high resolution imaging of fine structures such as dendrites and even dendritic spines with deep sample penetration by light (2). In addition, by utilizing a very small excitation volume, multiphoton imaging eliminates photodamage out of the focal plane, allowing for long-term functional imaging experiments such as monitoring of Ca<sup>2+</sup> transients in dendritic spines (3).

Typically, those wishing to perform MPLSM have been left with the option of purchasing an off-the-shelf commercial system or building a “do-it-yourself” custom system utilizing an existing confocal scanhead(4–6). Often more affordable and flexible, custom-built systems have required a level of technical expertise and programming beyond that of a typical biologist. Additionally, even after design, assembly, and testing by an experienced optical engineer, these setups almost always require constant surveillance and tweaking by the original designer and are prone to software glitches. The presented setup can be assembled, maintained, and utilized by any microscopists requiring multiphoton imaging capability.

### Materials and Methods

A schematic of the converted system is shown in Fig.1a. We have directly coupled a femtosecond pulsed NIR laser (Chameleon, Coherent) to the scanhead to provide

multiphoton excitation. This external excitation beam is attenuated by an adjustable neutral density filter (5215, New Focus). In order to overfill the back focal aperture (BFA) of the objective lens, the beam diameter is expanded about three times by a telescope consisting of 50 mm and 150 mm focal length lenses placed sequentially in the beam path. The expanded beam is directed into the scanhead (C1, Nikon) by using a mirror insert (C50299, Nikon) equipped with a silver surface full mirror (21010, Chroma) to replace the dichroic mirror insert employed in the original confocal configuration (inset of Fig. 1a). The external optics (Microbench, Linos) are connected to the scanhead through a custom-made adapter plate that bolts directly to the scanhead after removal of the plastic clam-shell case utilizing existing clearance holes. The design of the adapter plate permits easy access to the mirror insert, which must be exchanged for switching between multiphoton and confocal modes (Fig. 1b). The original C1 scan mirrors direct the excitation beam to the objective lens (e.g. 40× water immersion, Fluor, Nikon). The back focal aperture of this lens receives ~85% of the laser power entering the scan head, as directly measured by a power meter (Lasermate 1, Coherent). In order to determine the effect of group velocity dispersion (GVD) in our system, we measured the autocorrelated pulse length of the beam (MINI Special, APE). All measurements were subjected to a lowpass filter and are the average of at least 4 measurements. The full width half maxima (FWHM) before and after the scanhead were 204fsec and 246fsec, respectively. This 25% increase in pulse length shows that the silver mirrors included in the scanhead are appropriate for multiphoton scanning.

In order to explore the feasibility of using acousto-optic modulation as an automated mechanism to modulate beam intensity as sample depth changes we inserted a 2mm aperture acousto-optic deflector (AOD) (LS55, Isomet) into the unexpanded beam path, which increased the measured pulse length by 30% to 318fsec. Spatial dispersion introduced by the AOD can be compensated by substituting a diffraction grating for one of the full mirrors in the beam path (7). The expected 30% loss in laser power is of no consequence for *in vitro* imaging as all presented samples are imaged with a neutral density filter of at least OD 1.5. The AOD can be controlled using the Nikon C1 software through use of an analog to digital converter (PCI-6035e, National Instruments).

Because of the highly local excitation volume, multiphoton imaging does not require spatial filtering by a confocal pinhole (8–10). Therefore, multiphoton-excited epifluorescence is not returned to the scanhead for descanning and spatial filtering by the pinhole, but rather is directly detected. The collection optics are located as close to the BFA of the objective as possible to maximize collection efficiency. For this purpose, an epifluorescence slider (Y-FL, Nikon) was added to the microscope, equipped with a custom filter cube (MPC) holding a long pass dichroic mirror (770dcxr, Chroma) to direct the collected fluorescence away from the scanhead and towards the external detector unit (Fig. 1c). This design allows convenient switching between the multiphoton detection pathway and the original confocal configuration. Most importantly, no modification to the C1 scanhead or the epifluorescence slider is needed. Collected fluorescence is sent through a focusing cube (FLC) containing two sequentially placed corrected achromats of 35 and 75mm focal length. This previously described lens system transmits >70% of the collected epifluorescence (11) through an infrared blocking filter (BG39, Schott) into a multimode fiberoptic cable (1.5mm aperture, ThorLabs). We mounted the optical cable through a 25mm SMA connector on an X-Y positioner (Microbench, Linos) which slides as shown on microbench rails along the Z axis to allow easy adjustment for maximum transmission of emission light. For uncaging experiments which require shorter excitation wavelengths, the 770nm longpass dichroic (Figure 1, MPC) can be easily substituted with a dichroic mirror of shorter wavelength.

We connected the fiberoptic cable to the original three-PMT detection unit (3 detector unit S, Nikon) of the C1 confocal microscope through its SMA connector. Use of the C1

detection unit allows for easy adaptation for various fluorophore combinations due to its exchangeable modular filter cubes.

Imaging can be performed using the standard imaging software (EZ-C1 Version 2.1, Nikon) provided with the confocal system, without modification to operate the scan mirrors, axial positioning of the objective lens, and PMT parameters. Wavelength and emission of the NIR laser can be controlled either directly on the front panel of the laser power supply or using the provided software interface (Chameleon, Coherent).

Images were processed using both the Nikon EZ-C1 software as well as ImageJ software, freely available through NIH. For point spread function (PSF) approximation, a 3-D stack of images of a sub-resolution diameter fluorescent bead was acquired, and intensity values measured along a single axis were plotted versus distance and fit to a Gaussian distribution (Origin 6.0, Microcal).

Exact technical specifications of custom made parts (highlighted in yellow) are available on request.

## Results

In order to evaluate the two-photon performance of the modified microscope, we chose to image different types of fluorescently labeled pollen grains (Carolina Biological Supply), producing optical sections at 2  $\mu\text{m}$  axial steps. Fig.2a shows six consecutive optical sections taken from an Alexa 488-labeled spiky grain, illustrating the imaging capability of the modified system. Fig.2b is a maximum projection image of another, dual-labeled, lobular pollen grain, reconstructed from two-photon excited fluorescence gathered in the first (green) and second (red) emission channels. Next, in order to determine the two-photon resolution of our microscope, we imaged subresolution fluorescent beads (180nm, Molecular Probes) mounted on poly-D-lysine coated glass cover slips using an excitation wavelength of  $\lambda=840\text{nm}$  and an objective lens of  $\text{NA}=0.8$  (Fig.2c). The full width at half maximum (FWHM) fluorescence intensity in both axial and lateral planes was determined as an approximation of the point spread function (PSF). The experimentally obtained value of  $\text{FWHM}_{\text{axial}} = 2.6 \mu\text{m}$  is a good match to the theoretical value  $\text{FWHM}_{\text{axial}} = 2 \mu\text{m}$  (12). Because the diameter of the bead approaches half of the theoretical excitation PSF of  $\text{FWHM}_{\text{lateral}} (388.5\text{nm})$  its effect on the observed image was taken into account. Convolution of our theoretical Gaussian PSF with a sphere of 180 nm diameter yields a theoretical image of just over 400 nm FWHM in the lateral plane, comparable to our measured  $\text{FWHM}_{\text{lateral}}$  of 500nm.

Finally, to demonstrate the effectiveness of the modified microscope for imaging of live tissue, we imaged mouse neuronal tissue. For structural imaging, whole retinas were extracted from heterozygous knock-in mice expressing a human rhodopsin-EGFP fusion protein (13). The tissue was imaged in artificial cerebrospinal fluid with a  $512 \times 512$  pixel scan pattern and a 2.6  $\mu\text{s}$  pixel dwell time. The excitation power at the BFA of a  $40\times$  (NA 0.8) water immersion objective lens (Fluor, Nikon) was approximately 30mW at 840nm (Fig.3a). The images reveal fluorescence in clearly observed individual photoreceptor cell outer segments (1.4  $\mu\text{m}$  diameter) where the rhodopsin protein localizes, which corresponds nicely to similar images taken on the C1 using the confocal configuration (Fig. 3b) with the smallest pinhole (30  $\mu\text{m}$ ).

In order to demonstrate the capacity to conduct functional imaging experiments, striatal brain slices were prepared from C57 mice. Individual neurons were whole-cell patched and dialyzed with standard internal solution containing 200  $\mu\text{M}$  of the fluorescent calcium indicator dye Oregon Green BAPTA-1 (OGB-1) and 50  $\mu\text{M}$  of the fluorescent label Alexa

Fluor 594. Imaging was performed using a 100× (NA 1.1) water immersion objective (Plan, Nikon) and approximately 12mW BFA average power at 810nm excitation. Dendritic structures of a striatal spiny neuron are presented in Fig.3c as a maximum projection image generated from a series of optical sections separated by 0.5 μm. During functional imaging, a train of 15 action potentials was induced by injecting depolarizing current into the soma in current clamp mode. Calcium influx was determined as the increase of OGB-1 fluorescence normalized by its resting fluorescence ( $\Delta F/F$ ) throughout the course of a linescan through a single spine (Fig.3c inset). No significant bleaching or obvious photodamage was observed throughout the course of imaging. The low laser power used as well as the good signal-to-noise ratio of the  $Ca^{2+}$  signal observed from easily discernible distal dendritic spines illustrate that our modified laser scanning microscope can be used effectively for functional imaging experiments with multiphoton excitation.

## Conclusion

We have presented here a straightforward and effective multiphoton adaptation of a common commercial confocal microscope that allows rapid switching between confocal and multiphoton modes. The entire conversion requires no modification of the original system and only a few custom-made parts. The previously demonstrated efficient fiber optic coupling of epi-fluorescence emission (11), to the C1 detection unit allows for convenient simultaneous probing of multiple fluorophores that can quickly be changed using the modular filter cubes present in this unit. The imaging software of the original confocal system can be used without any modifications for multiphoton imaging.

The presented microscope is ideal for biological imaging applications and could be modified by users with little or no mechanical or electronics experience. Except for the pulsed NIR laser, the components used are relatively inexpensive and widely available. We have demonstrated the system's utility by imaging fluorescent proteins and indicator dyes of a number of different excitation and emission wavelengths in two different neuronal preparations. This versatile microscope can be utilized by groups that lack either the resources to purchase a pre-packaged system or the technical know-how to build a new system from scratch.

## Acknowledgments

The presented work was supported by NIH training grant EY T32 EY07102 (JJM), NIH grants R01-EY11900 and R01-DA015189 and Welch Foundation Q0035 (TGW) as well as NIH-NIA/RO1 AG027577 and NSF/DBI-0455905 (PS).

## Reference List

1. Denk W, Strickler JH, Webb WW. *Science*. 1990; 248:73–76. [PubMed: 2321027]
2. Svoboda K, Yasuda R. *Neuron*. 2006; 50:823–839. [PubMed: 16772166]
3. Denk W, Yuste R, Svoboda K, Tank DW. *Current Opinion in Neurobiology*. 1996; 6:372–378. [PubMed: 8794079]
4. Majewska A, Yiu G, Yuste R. *Pflugers Archiv-European Journal of Physiology*. 2000; 441:398–408. [PubMed: 11211128]
5. Soeller C, Cannell MB. *Pflugers Archiv-European Journal of Physiology*. 1996; 432:555–561. [PubMed: 8766017]
6. Ridsdale A, Micu I, Stys PK. *Appl.Opt.* 2004; 43:1669–1675. [PubMed: 15046170]
7. Iyer V, Losavio BE, Saggau P. *Journal of Biomedical Optics*. 2003; 8:460–471. [PubMed: 12880352]
8. Piston DW, Wu ES, Webb WW. *Faseb Journal*. 1992; 6:A34.

9. Piston DW, Kirby MS, Cheng HP, Lederer WJ, Webb WW. *Applied Optics*. 1994; 33:662–669. [PubMed: 20862061]
10. Denk W, Detwiler PB. *Proceedings of the National Academy of Sciences of the United States of America*. 1999; 96:7035–7040. [PubMed: 10359834]
11. Larson, A.; Iyer, V.; Hoogland, T.; Saggau, P. Fiber-coupled non-descanned 4 pi detection with a commercial confocal microscope modified for multiphoton imaging. Periasamy, Ammasi; Peter, TCS., editors. Vol. 4963. SPIE; 2003. p. 239-251. Ref Type: Conference Proceeding
12. Williams RM, Piston DW, Webb WW. *Faseb Journal*. 1994; 8:804–813. [PubMed: 8070629]
13. Chan F, Bradley A, Wensel TG, Wilson JH. *Proceedings of the National Academy of Sciences of the United States of America*. 2004; 101:9109–9114. [PubMed: 15184660]

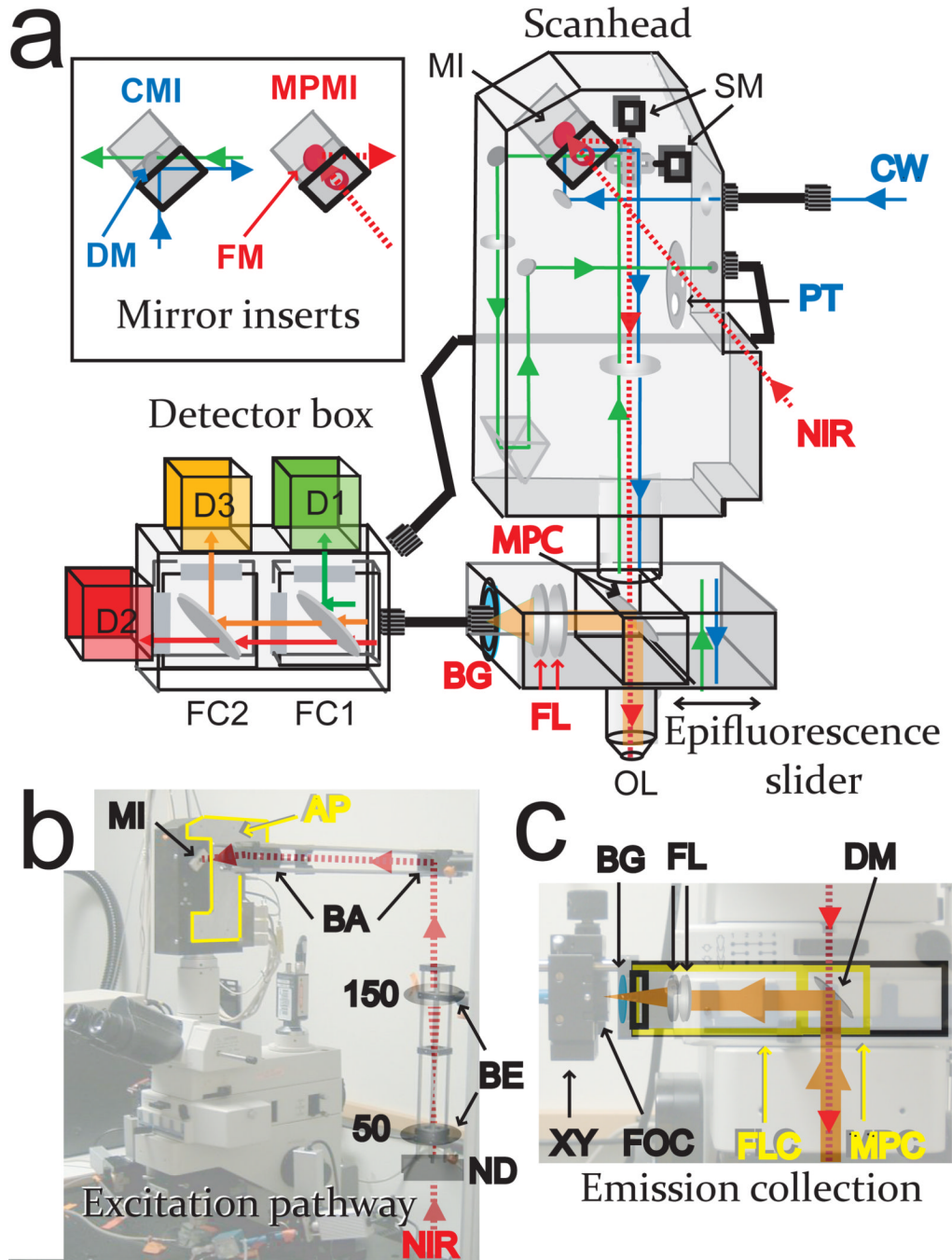


**Figure 1.** Confocal to multiphoton conversion. **(a)** Schematic of system adaptation. The near infrared (NIR) excitation path is shown in red, multiphoton-excited emission in orange, CW excitation in blue, and standard single photon-excited emission in green. Components utilized in both configurations are labeled black, in confocal only blue, and in multiphoton only red. The setup is shown in the multiphoton configuration, where the detector unit is connected by multimode fiber optic cable to the epifluorescence slider and not the scanhead. Abbreviations: mirror insert (MI), scan mirrors (SM), pinhole turret (PT), multiphoton cube (MPC), focusing lens (FL), blue glass filter (BG), objective lens (OL). Inset: Confocal

mirror insert (CMI) using dichroic mirror (DM), multiphoton mirror insert (MPMI) using full mirror (FM). Detector: emission filter cubes (FC1,2), and detectors (D1,2,3). **(b)** Multiphoton excitation pathway with NIR beam passing neutral density filter (ND), telescoping beam expander (BE) consisting of 50 and 150mm focal length achromats, and beam aligner (BA) before entering custom-made mirror insert (MI). Also shown is the custom-made adapter plate (AP) (highlighted in yellow) connecting the scan head to the external optics. **(c)** Multiphoton epi-fluorescence emission pathway. Two special cubes were connected to the rail inside the slider by means of its dovetail and clamping screws: A custom-made focusing cube (FLC, highlighted in yellow) was secured to the leftmost (as shown) part of the rail. This cube contains the 17.5mm focal length lens combination (FL) and the 25mm diameter tube that serves to anchor the microbench parts holding the BG39 emission filter, (BG), X–Y positioner (XY), and fiberoptic coupling (FOC). The multiphoton cube (MPC, highlighted in yellow) containing the dichroic mirror (DM) is oriented such that the collected fluorescence is directed away from the scanhead and towards the external detector unit, is then fastened to the same rail immediately adjacent to the focusing cube. The slider is placed in position 2 (as shown) for multiphoton microscopy and position 1 to remove the dichroic mirror from the beam path in confocal mode.

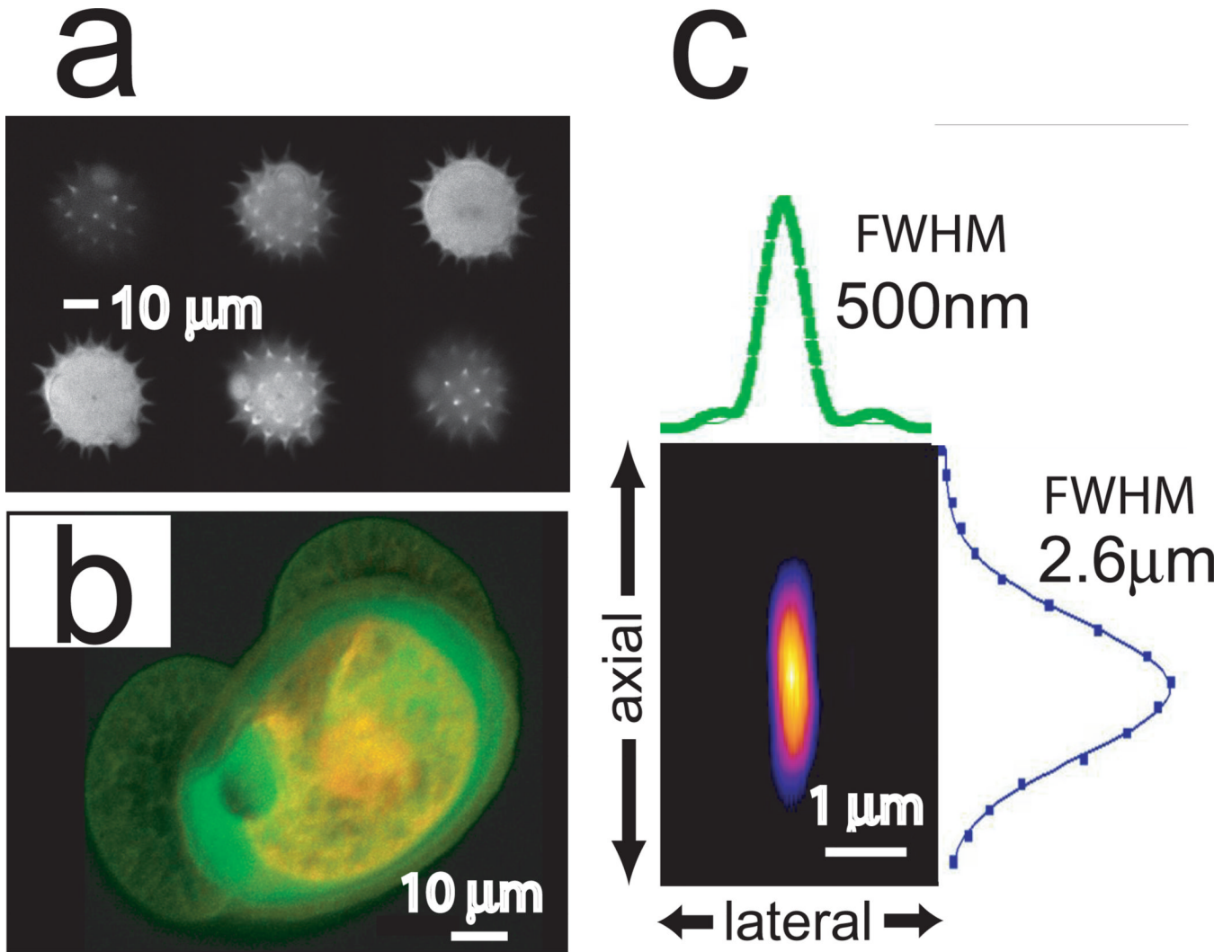


**Figure 2.**

Two-photon performance of modified microscope. (a)  $6 \mu\text{m}$  optical sections of two-photon excited fluorescence from an Alexa 488 labeled pollen grain. (b) Maximum projection image constructed from a stack of  $1 \mu\text{m}$  optical sections of two-photon excited fluorescence from a pollen grain labeled with Alexa 488 (green) and Alexa 594 (red). (c) False color image z-plane reconstruction made from two-photon images of a subresolution bead ( $180\text{nm}$ , Alexa 488). Shown are intensity profiles for the x and z planes along with the FWHM of intensity. Not shown y-axis FWHM =  $460\text{nm}$ .



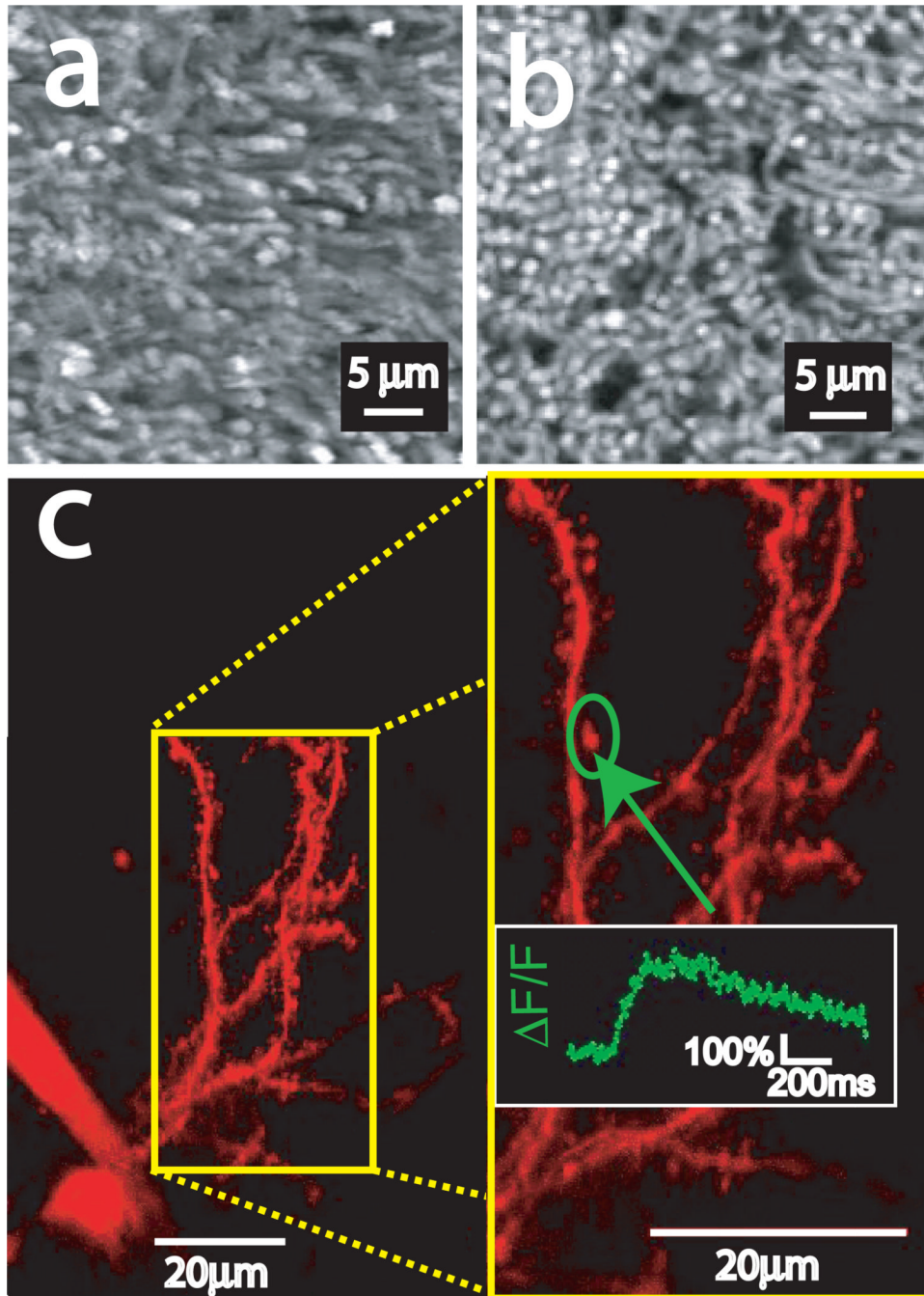


**Figure 3.**

(a) Maximum projection of two-photon fluorescence images of a single Rhodopsin-EGFP expressing retina taken in multiphoton mode with no spatial filtering. (b) Maximum projection of single photon fluorescence images of a single Rhodopsin-EGFP expressing retina taken in confocal mode and filtered through the 30 μm (smallest) pinhole. (c) Two-photon images using a 100× water immersion objective (NA=1.1) of a mouse striatal neuron in a brain slice filled with Alexa 594 and OGB-1. Inset is a 2× zoom of the area bounded by the yellow box. Graph is the normalized change in OGB-1 fluorescence ( $\Delta F/F$ ) in the

circled dendritic spine in response to a train of action potentials, measured in line scan mode.